Standardized Shrinking LORETA-FOCUSS (SSLOFO): A New Algorithm for Spatio-Temporal EEG Source Reconstruction

Hesheng Liu, *Member, IEEE*, Paul H. Schimpf*, *Member, IEEE*, Guoya Dong, Xiaorong Gao, Fusheng Yang, and Shangkai Gao, *Senior Member, IEEE*

***Abstract*—This paper presents a new algorithm called Standardized Shrinking LORETA-FOCUSS (SSLOFO) for solving the electroencephalogram (EEG) inverse problem. Multiple techniques are combined in a single procedure to robustly reconstruct the underlying source distribution with high spatial resolution. This algorithm uses a recursive process which takes the smooth estimate of sLORETA as initialization and then employs the re-weighted minimum norm introduced by FOCUSS. An important technique called standardization is involved in the recursive process to enhance the localization ability. The algorithm is further improved by automatically adjusting the source space according to the estimate of the previous step, and by the inclusion of temporal information. Simulation studies are carried out on both spherical and realistic head models. The algorithm achieves very good localization ability on noise-free data. It is capable of recovering complex source configurations with arbitrary shapes and can produce high quality images of extended source distributions. We also characterized the performance with noisy data in a realistic head model. An important feature of this algorithm is that the temporal waveforms are clearly reconstructed, even for closely spaced sources. This provides a convenient way to estimate neural dynamics directly from the cortical sources.**

***Index Terms*—EEG, inverse problem, spatio-temporal analysis.**

I. Introduction

As a noninvasive brain imaging technique, the electroencephalogram (EEG) can directly reflect neuronal activity with high temporal resolution but poor spatial resolution. In order to obtain more detailed spatial information, a mathematical procedure referred to as the "inverse problem" can be applied to estimate the underlying cortical sources. A popular approach to address the inverse problem is dipole source localization, which assumes one or multiple current dipoles to represent the electric sources, and attempts to determine the locations, magnitudes, and perhaps the orientation of these dipoles [1]–[5]. The use of a few equivalent dipole sources is considered to be appropriate in modeling epileptic foci or other very focal activities. However, most dipole methods require correct estimation of the number of sources [6], [7]. In recent years, another approach termed distributed source model has been widely studied [8]–[10]. Distributed source models do not limit the number of sources, nor do they necessarily restrict the sources to be dipolar. This approach can easily take advantage of anatomical or physiological information provided by other imaging modalities such as functional magnetic resonance imaging [11].

Distributed source models make a determination of source activity at every possible location. This leads to a highly underdetermined and ill-posed problem with multiple solutions. A cost function is generally defined in order to choose a particular solution, and both linear and nonlinear optimization methods have been used to find the minimum of that cost function. Different cost functions may choose different solutions, so the most appropriate cost function is application-specific. A thorough analysis of the theoretic basis of various inverse algorithms has been given by Mosher *et al.* [12]. Among these approaches, weighted minimum norm (WMN) methods have proven to give promising results [13]. One well-known WMN method is the low-resolution electromagnetic tomography (LORETA) algorithm [8], [9]. This algorithm introduces a Laplacian operator into the weighting matrix to obtain a "neurophysiologically smooth solution." Recently, Pascual-Marqui developed a new algorithm termed standardized LORETA [14]. Although sLORETA sounds like an updated version of LORETA, the basic idea is quite different from that of applying a spatial smoothing operator, as in LORETA. Instead, sLORETA uses the resolution matrix to normalize a coarse WMN estimation, and can thereby correctly reconstruct single sources on noise-free data. Details of this algorithm will be covered in the Section II of this paper. Nevertheless, both LORETA and sLORETA generate source distributions with low spatial resolution. Although it is possible to correctly localize sources by finding well separated maxima in the image, these low-resolution approaches can exhibit poor performance in recovering multiple sources when the point-spread functions (PSF's) of the sources overlap. When measurements are contaminated by noise, the inverse procedure must employ a regularization

Manuscript received June 22, 2004; revised December 23, 2004. This work was supported in part bby the National Science Foundation (NSF) under Grant 0112742 and in part by the National Natural Science Foundation of China under Grant 60318001. *Asterisk indicates corresponding author*.

H. Liu is are with the School of Electrical Engineering and Computer Science, Washington State University, Spokane, WA 99202 USA (e-mail: heshengliu@yahoo.com).

*P. H. Schimpf is with the School of Electrical Engineering and Computer Science, Washington State University, Spokane, WA 99202 USA (e-mail: schimpf@ wsu.edu).

G. Dong is with the Province-ministry Joint Key Laboratory of Electromagnetic Field and Electrical Apparatus Reliability, Department of Electrical Engineering, Hebei University of Technology, Tangshan 063009, China.

X. Gao, F. Yang and S. Gao are with the Department of Biomedical Engineering, Tsinghua University, Beijing 100084, China.

Digital Object Identifier 10.1109/TBME.2005.855720

technique to avoid unstable solutions due to the ill-posed nature of the EEG inverse. Regularization tends to increase the spatial blurring of LORETA and sLORETA solutions. Specialized cost functions can be defined to improve the spatial resolution. Some studies replace the L2-norm of the WMN methods by the L1-norm [10]. A hybrid approach which incorporates L1-norm with L2-norm has also been introduced by Uutela *et al.* [15]. However, minimizing the L1-norm generally requires much more computational effort than minimizing the L2-norm.

One promising high-resolution algorithm is the focal underdetermined system solver (FOCUSS) [16], [17]. This algorithm is a WMN method that makes recursive adjustments to the weighting matrix until most elements of the solution are close to zero. It has been proven to converge to a sparse solution with no more nonzero sources than the number of sensors. FOCUSS is appropriate for recovering a few focal sources, but relies on a robust initialization. In [16], an unbiased minimum norm was used as the initial estimate for FOCUSS.

For a local optimizer, only a correct initialization can assure that the algorithm starts in the correct basin of attraction. We previously proposed a recursive algorithm called Shrinking LORETA-FOCUSS, which uses a LORETA solution as the initialization for a recursive algorithm similar to FOCUSS [18], [19]. Although Shrinking LORETA-FOCUSS has much better performance compared to FOCUSS, neither of these methods is able to accurately recover the time series of the source activities. FOCUSS is basically a WMN method but it constructs weighting matrix based on the source estimation and, thus, it applies different weighting matrices at different time samples. Shrinking LORETA-FOCUSS recursively reduces the source space so it has different source spaces for different time samples. These nonlinear factors hamper the application of these two algorithms in time series analysis.

There is now common agreement that electric activity in the brain is organized in functional regions that synchronize in a cooperative way. Thus, a spatio-temporal pattern analysis is very desirable in brain research. Analysis of cortical sources demands an inverse method with capabilities beyond source distribution in the brain, but one that can also reveal the temporal process of these sources. There exist different ways to employ temporal information in an inverse calculation. Some dipole methods assume the sources are spatially fixed during a time segment and, thus, factor out the temporal information as linear parameters and iteratively search for sources in the space domain [4], [5]. Another widely used approach is the linearly constrained minimum variance method which also assumes a stationary source distribution in a given epoch and employs the covariance of the measurements to form the optimization criterion [20]. A recent work of Schmitt *et al.* suggested "temporal smoothness" of the sources can be taken as an *a priori* constraint in source localization [21]. This additional constraint can be conveniently incorporated in the regularization of inverse problems.

In this paper, we present an algorithm that we refer to as Standardized Shrinking LORETA-FOCUSS (SSLOFO). This algorithm aims at localizing the sources with relatively high spatial resolution and estimating the time series for each source. A simple re-weighting strategy has been used to incorporate the temporal information and retains the linearity of the algorithm. SSLOFO is capable of recovering single or multiple sources with their temporal waveforms and performs well with noisy data. These advantages make this algorithm a promising tool for human brain mapping. Simulation results in both spherical and realistic head models are shown in Section III. For interested readers, code to implement SSLOFO is available upon request to the corresponding author.

II. Methdology

A. Standardized Loreta Algorithm

The distributed source localization problem can be stated as

$$\mathbf{\Phi} = \mathbf{KJ} \tag{1}$$

where $\mathbf{\Phi}$ is an $N \times 1$ vector containing the electric potentials from electrodes on the scalp, $\mathbf{J}$ is a $3M \times 1$ vector representing current sources at M locations within the brain volume, with three orthogonal components per location, and $\mathbf{K}$ is the lead-field matrix representing the system transfer coefficients from each source to each measuring point. A unique solution to (1) can be achieved by zero-order Tikhonov-Philips regularization, which uses the following cost function:

$$\min_J \{||\mathbf{\Phi} - \mathbf{KJ}||^2 + \alpha ||\mathbf{J}||^2\} \tag{2}$$

where α is the regularization parameter determined by the discrepancy principle or using the L-curve method [22]. The source estimation is then derived as

$$\hat{\mathbf{J}} = \mathbf{T}\mathbf{\Phi} \tag{3}$$

where

$$\mathbf{T} = \mathbf{K^T}[\mathbf{K}\mathbf{K}^T + \alpha\mathbf{I}]^{-1}. \tag{4}$$

Substituting (1) into (3) yields

$$\hat{\mathbf{J}} = \mathbf{TKJ} = \mathbf{K^T}[\mathbf{K}\mathbf{K}^T + \alpha\mathbf{I}]^{-1}\mathbf{KJ} = \mathbf{RJ} \tag{5}$$

where $\mathbf{R}$ is the resolution matrix, defined as

$$\mathbf{R} = \mathbf{K^T}[\mathbf{K}\mathbf{K}^T + \alpha\mathbf{I}]^{-1}\mathbf{K}. \tag{6}$$

The resolution matrix describes a mapping from the actual source activity to the estimated activity. Ideally, $\mathbf{R}$ would be an identity matrix. In actuality, it cannot be identity because of the ill-posed nature of the inverse problem. Note that the rank of the resolution matrix cannot exceed the rank of the lead field matrix $\mathbf{K}$ and $\mathbf{K}$ is ill-posed, therefore, $\mathbf{R}$ is not invertible. The basic idea of sLORETA is to normalize the estimation using a block-by-block inverse of the resolution matrix $\mathbf{R}$, as follows:

$$\hat{\mathbf{J}}_l^T(\mathbf{R}_{ll})^{-1}\hat{\mathbf{J}}_l \tag{7}$$

where $\hat{\mathbf{J}}_l$ is a 3×1 vector containing the source estimate at the lth voxel (3) and $\mathbf{R}_{ll}$ is a 3×3 matrix containing the lth diagonal block of the resolution matrix. It has been shown that sLORETA can correctly localize a single source [14]. Though the image produced by sLORETA is blurred, the summit of the image is correctly centered at the location of the source.

B. Standardized FOCUSS Algorithm

FOCUSS is a high-resolution algorithm that recursively implements the WMN method and converges to a sparse solution [16], [17]. From the introduction of sLORETA we know that the localization performance of a minimum norm method is highly improved by the standardization process. Since each step of FOCUSS represents a WMN inverse, it is reasonable to apply standardization there as well. In this study, we investigated the efficacy of such standardization. In FOCUSS, the solution to (1) is achieved as follows:

$$\min_{\mathbf{J}} ||\mathbf{CJ}||^2, \text{ subject to } \mathbf{\Phi} = \mathbf{KJ} \tag{8}$$

where $\mathbf{C}$ is the weighting matrix defined as

$$\mathbf{C} = (\mathbf{W}^{-1})^T\mathbf{W}^{-1} \tag{9}$$

$\mathbf{W}$ is a diagonal $3M \times 3M$ matrix which is recursively refined. The solution to (8) at the ith iteration is

$$\begin{aligned}\hat{\mathbf{J}}_i &= \mathbf{C}_i^{-1}\mathbf{K}^T\left[\mathbf{K}\mathbf{C}_i^{-1}\mathbf{K}^T\right]^+\mathbf{\Phi} \\ &= \mathbf{W}_i\mathbf{W}_i^T\mathbf{K}^T\left(\mathbf{K}\mathbf{W}_i\mathbf{W}_i^T\mathbf{K}^T\right)^+\mathbf{\Phi}\end{aligned} \tag{10}$$

where "+" denotes the Moore-Penrose pseudo-inverse. At each iteration, the matrix $\mathbf{W}$ is updated based on the current density estimated by the previous step, as follows:

$$\mathbf{W}_i = \mathbf{P}\mathbf{W}_{i-1}[Diag(\hat{\mathbf{J}}_{i-1}(1), \hat{\mathbf{J}}_{i-1}(2), \ldots, \hat{\mathbf{J}}_{i-1}(3M))] \tag{11}$$

where $\hat{\mathbf{J}}_{i-1}(n)$ represents the nth element of vector $\hat{\mathbf{J}}$ from the previous iteration. $\mathbf{P}$ is a diagonal matrix that compensates for deep sources

$$\mathbf{P} = Diag\left[\frac{1}{||\mathbf{K}_1||} \cdots \frac{1}{||\mathbf{K}_{3M}||}\right] \tag{12}$$

where $||\mathbf{K}_i||$ denotes the ith column of $\mathbf{K}$. The FOCUSS algorithm converges to a localized solution with zero contribution from most sources. Inspired by the localization performance of sLORETA, we incorporated standardization into the FOCUSS algorithm as well. Substitution of (1) into (10) yields

$$\hat{\mathbf{J}}_i = \mathbf{W}_i\mathbf{W}_i^T\mathbf{K}^T\left[\mathbf{K}\mathbf{W}_i\mathbf{W}_i^T\mathbf{K}^T\right]^+\mathbf{KJ} = \mathbf{R}_i\mathbf{J}. \tag{13}$$

So the resolution matrix in the ith step is

$$\mathbf{R}_i = \mathbf{W}_i\mathbf{W}_i^T\mathbf{K}^T\left[\mathbf{K}\mathbf{W}_i\mathbf{W}_i^T\mathbf{K}^T\right]^+K. \tag{14}$$

The power of the source estimation in the ith step is then normalized as

$$\hat{\mathbf{J}}_i^T(l)[\mathbf{R}_i(l,l)]^{-1}\hat{\mathbf{J}}_i(l) \tag{15}$$

where subscript i is the index of iteration, $\hat{\mathbf{J}}_i(l)$ is the source estimation at the lth voxel given by (10), and $[\mathbf{R}_i(l,l)]$ is a 3×3 matrix containing the lth diagonal block of the resolution matrix. This standardized FOCUSS is very similar to FOCUSS, except that the source estimate is normalized by the resolution matrix to correct the bias. We have found that this significantly improves the localization performance.

C. Single Time Point SSLOFO

Like FOCUSS, standardized FOCUSS is highly dependent on the initialization. The algorithm starts from some initial estimate and converges to an optimal solution near the initialization. It has been suggested that an ideal initialization of FOCUSS would be a low-resolution image of the true sources [16], [19]. In [19], LORETA has been successfully employed to initialize FOCUSS. In this paper, we use the same strategy of using a low-resolution method to initialize a high-resolution method. However, both the initialization method and the re-weighting process are improved. We initialize standardized FOCUSS using sLORETA, which results in an algorithm which has much better performance than Shrinking LORETA-FOCUSS.

Although a proper initialization can improve the final solution estimated by standardized FOCUSS, there are still some potential problems that deserve careful consideration. FOCUSS is a re-weighted minimum norm method which creates an increasingly sparse solution during iteration. If some nodes do not contain any source activity, why not eliminate them from the solution space? Furthermore, if a particular node is incorrectly eliminated during some iteration, is there any possibility of bringing it back into the solution space? In [19], we developed the Shrinking LORETA-FOCUSS algorithm which attempts to address these problems. This algorithm shrinks the source space after each iteration of FOCUSS hence greatly reduces the computation load. A smoothing operation is employed to prevent the algorithm from producing over-focal solution. The smoothing operation is critical because it keeps the recursive process from being trapped in some local minima. It is equivalent to re-initializing the subsequent FOCUSS process with a "blurred" source image after each iteration. The efficacy of this smoothing strategy has been shown by simulation studies in [19].

We, therefore, propose an algorithm named Standardized Shrinking LORETA-FOCUSS (SSLOFO) that integrates the above techniques. The algorithm can be summarized as follows.

1) Estimate the current density $\hat{\mathbf{J}}_0$ using sLORETA.
2) Initialize the weighting matrix according to (9), with

$$\mathbf{W}_0 = Diag(\hat{\mathbf{J}}_0(1), \hat{\mathbf{J}}_0(2), \ldots, \hat{\mathbf{J}}_0(3M))]. \tag{16}$$

3) Estimate the source power using standardized FOCUSS according to (13) and (15).
4) Retain prominent nodes along with their neighboring nodes [19]. Adjust the values on these nodes through smoothing [19]. The selection of "prominent nodes" may be application-specific.
5) Redefine the solution space to contain only the retained nodes, i.e., retain only the corresponding elements in $\mathbf{J}$ and the corresponding columns in $\mathbf{K}$.
6) Update the weighting matrix according to (11).
7) Repeat the steps (3)–(6) until a stopping condition is satisfied, as discussed below.
8) Let the solution of the last iteration before smoothing be the final solution.

The iterations are stopped when: a) the solution does not change in two consecutive steps, or b) the solution of any iteration is less sparse than the solution estimated by the previous iteration, or c) the source strength of any node exceeds a threshold preset by the user. The first criterion indicates that the algorithm has converged to a fixed solution. The second criterion safeguards the algorithm from growing the solution space during Step 4, which could otherwise result in nontermination or oscillation. The third criterion is optional and it enables the user to stop the iteration earlier according to the need of a specific application. This can avoid the production of an over-focal solution when it is physiologically unreasonable. Such a flexible strategy is especially useful in some experimental human research.

D. Spatio-Temporal SSLOFO

When time series are considered, the basic function in (1) can be rewritten as

$$\mathbf{\Phi}_t = \mathbf{K}\mathbf{J}_t \tag{17}$$

where the subscript t is the index of time samples.

Because of their nonlinear features, FOCUSS and Shrinking LORETA-FOCUSS are not capable of estimating the temporal waveforms of the spatially fixed sources. They can localize a source at some place very close to the true position; however, at a different time the source may be localized to a different location, though the localization error could still be very small. The recovered time series at a given location may, therefore, be discontinuous.

One way to integrate temporal information is to assume that the sources are spatially fixed during a short time window and, thus, the linear temporal information can be factored out [5]. Based on this assumption, the single time point SSLOFO can easily be adapted to a spatio-temporal version

1) For a given time window, at each time sample t an inverse solution $\hat{\mathbf{J}}_t$ is calculated by single time point SSLOFO.
2) Sum up all of these solutions in the time window to obtain $\mathbf{S} = \sum_t \hat{\mathbf{J}}_t$
3) Re-define the solution space to be nodes that have nonzero values in $\mathbf{S}$.
4) For each time sample in the window, re-calculate the inverse solution using the WMN method according to the following formula:

$$\hat{\mathbf{J}}_t = \bar{\mathbf{S}}\bar{\mathbf{S}}^T\bar{\mathbf{K}}^T\left(\bar{\mathbf{K}}\bar{\mathbf{S}}\bar{\mathbf{S}}^T\bar{\mathbf{K}}^T\right)^+\mathbf{\Phi}_t \tag{18}$$

where the weighting matrix $\bar{\mathbf{S}}$ and lead field matrix $\bar{\mathbf{K}}$ are derived from $\mathbf{S}$ and $\mathbf{K}$ by eliminating the nodes/columns other than the new solution space.

For each time sample, the source space and weight matrix $\bar{\mathbf{S}}$ are identical, thus, the algorithm is linear. Spatio-temporal SSLOFO is, thus, able to produce a continuous waveform at each source location. Although the solution in (18) is calculated using a low-resolution method (WMN), it still has very high spatial resolution because the solution space has been confined to a small area.

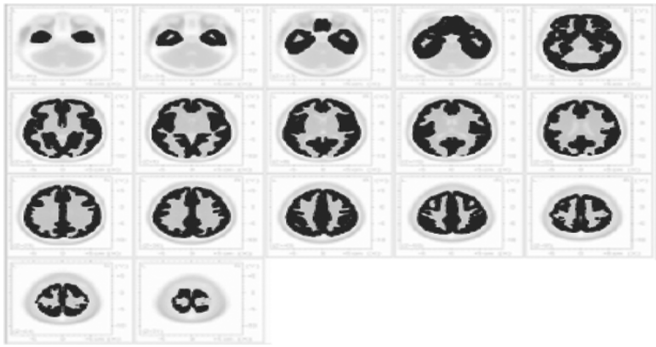

Fig. 1. The source space of the spherical head model (dark area). The upper-left slice is the lowest part of the brain; the lower-right slice is the topmost part of the brain.

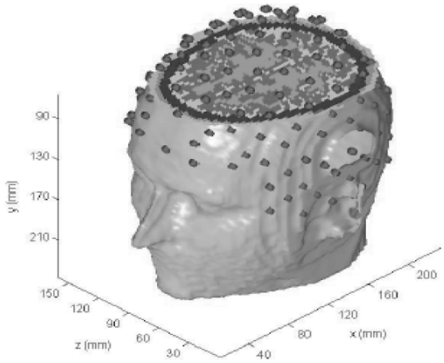

Fig. 2. The realistic head model, with cutaway illustrating classified tissues and superimposed EEG sampling points (dots).

III. Results

A. Head Models

To evaluate the SSLOFO algorithm, simulations were carried out in both a spherical and realistic head model. A spherical model has been widely adopted because of its simplicity. We chose to test SSLOFO in the spherical model so that the results can be compared with the results of other methods in the literature. However, we also desired a characterization of SSLOFO in a realistic geometry head model, and chose that model for our investigation into its performance with noisy measurements. This allowed us to evaluate the potential of this algorithm in experimental human research.

For a spherical model we chose the three-shell model [9] registered to the Talairach human brain atlas [23]. This model was kindly provided by Pascual-Marqui, R.D. The solution space was originally restricted to cortical gray matter and hippocampus, consisting of 2394 nodes at a 7-mm spatial resolution. Fig. 1 shows the solution space (dark area) along 17 horizontal slices through the brain. The measurement space consisted of 127 electrodes on the scalp. Our realistic head model is based on classified magnetic resonance images of a human head. The tissue is classified according to the method discussed in [24]. The model contained 11 tissue types with resistivities obtained from [25]. The lead-field matrix was calculated using the finite element method [26]–[28]. This model is illustrated in Fig. 2. The EEG observation contained 145 channels and the source space consisted of 3035 locations sampled from the cortical surface at a resolution of

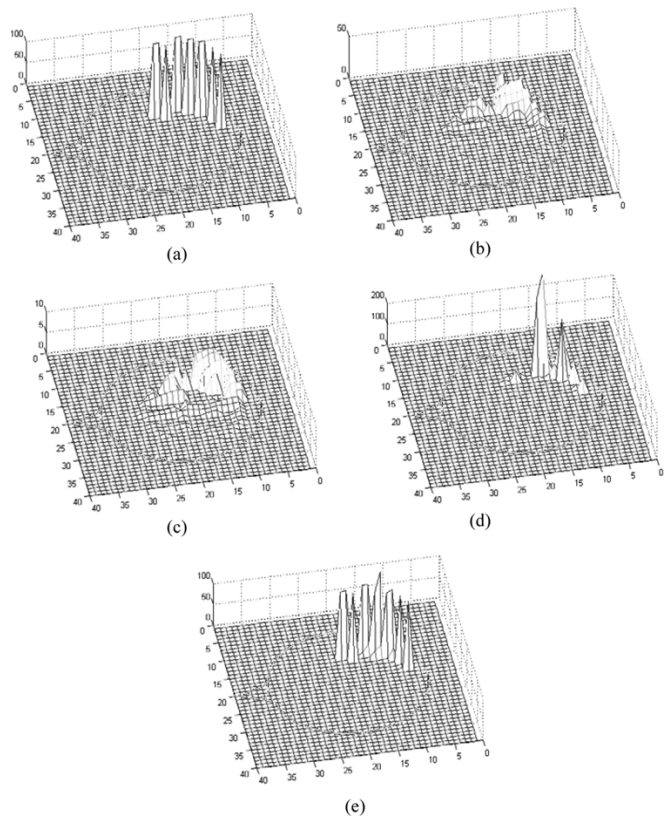

Fig. 3. Reconstruction of source distribution in shape of an arc (a) 11 simulated sources are located in shape of an arc (b) solution of WMN method; (c) solution of sLORETA; (d) solution of FOCUSS (e) solution of SSLOFO.

$4.0 \times 4.0 \times 3.2$ mm resolution, resulting in a lead field matrix of dimension 145×9105, with three orthogonal source directions per location.

B. Noise-Free Simulations

We compared four different inverse methods on the spherical model in the absence of noise: WMN, sLORETA, FOCUSS, and SSLOFO. We included WMN, FOCUSS, and sLORETA in this study because SSLOFO is derived from all of them, and we wished to give a clear impression of the improved performance that is possible with SSLOFO over each of them. Our weighting matrix for WMN was defined as in (9). Our implementation of FOCUSS used WMN as the initialization method, as suggested in [16]. The noise-free simulations attempt to reflect the localization ability of different algorithms so temporal courses are not considered in this section.

Our comparison begins with a complex source distribution. Fig. 3(a) shows 11 sources located in shape of an arc. Because the sources are located at the same depth within the brain, we show only the image of that slice. Fig. 3(b)–(e) illustrates the source images produced by WMN, sLORETA, FOCUSS, and SSLOFO, respectively. The arc is recovered to some extent by WMN, but the spatial resolution is very low [Fig. 3(b)]. The solution produced by sLORETA is more blurred, although the shape of the arc can still be perceived [Fig. 3(c)]. In the FOCUSS solution [Fig. 3(d)], some sources are lost and other sources become abnormally large, changing the shape of the distribution. The SSLOFO solution [Fig. 3(e)] is almost identical to the simulated distribution.

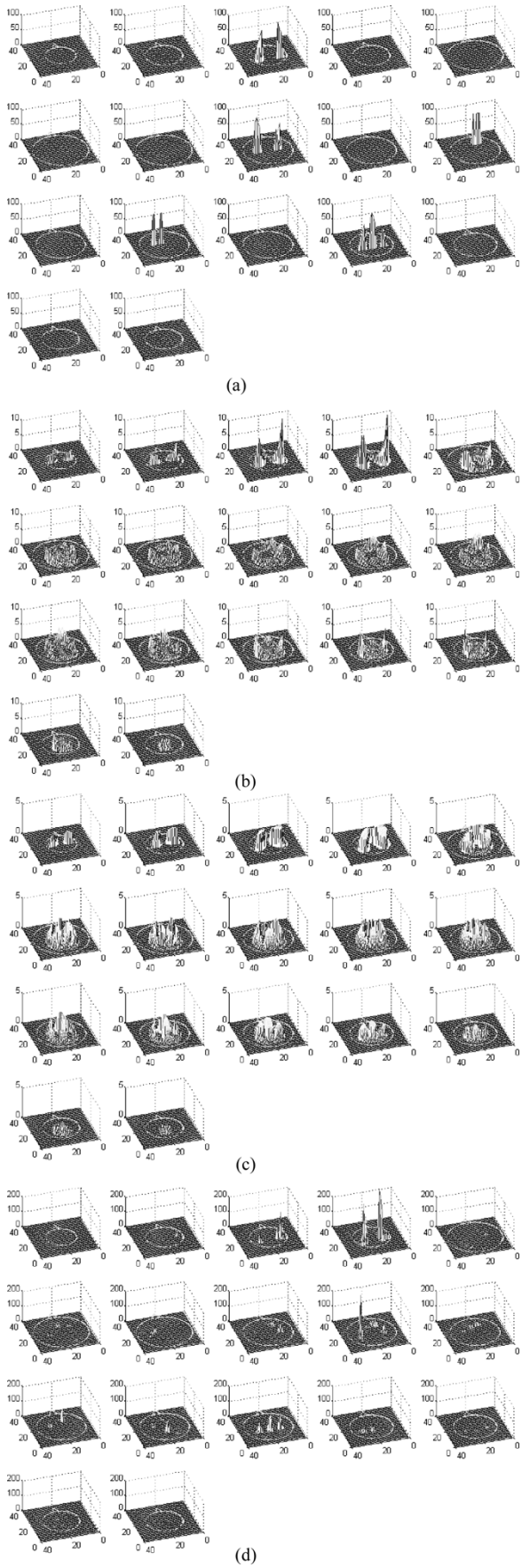

Fig. 4. Reconstruction of distributed source clusters by four different algorithms. (a) The simulated source configuration; (b) solution of WMN method; (c) solution of sLORETA; (d) solution of FOCUSS.

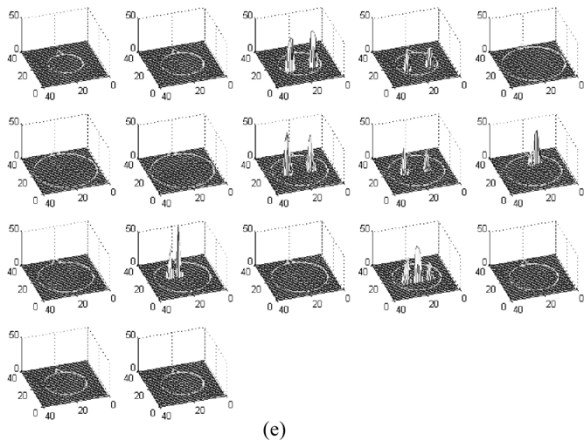

Fig. 4. *(Continued.)* Reconstruction of distributed source clusters by four different algorithms. (e) solution of SSLOFO.

Fig. 4(a) shows 10 source areas consisting of 41 single sources distributed in different areas of the brain. Fig. 4(b)–(e) displays sources reconstructed by four different algorithms, respectively. The WMN solution is quite different from the simulated configuration [Fig. 4(b)]. The image appears to be a distribution with the dominant activities in the third and fourth slices. The solution of sLORETA is so blurred [Fig. 4(c)] that the original source configuration can barely be seen. In the FOCUSS solution [Fig. 4(d)], many sources are absorbed and some large spurious sources appear. The solution of SSLOFO [Fig. 4(e)] is very similar to the simulated distribution except for some energy leakage into slices adjacent to the actual sources slices, which represents a small amount of spread. This simulation shows SSLOFO is capable of recovering a number of distributed groups of localized sources, while the other methods studied here have poor performance.

When the sources are few and clustered, high-resolution algorithms usually achieve better results compared to low-resolution algorithms. For example, dipole fitting methods such as MUSIC and R-MUSIC can localize several sources with small localization error [4], [5]. FOCUSS is also capable of reconstructing sparse sources. When the sources are large in number and extended, the performance of these high-resolution algorithms tend to suffer from some degradation. In such cases, a low-resolution algorithm such as LORETA or sLORETA may be a superior choice. As a combination of low- and high-resolution methods, SSLOFO can offer a way to achieve good results in both worlds, especially when the situation is mixed, i.e., distributed clusters of localized sources.

Fig. 5(a) shows a large number of sources (238 dipoles) in the temporal cortex, representing widespread activity in a specific area. Fig. 5(b) displays the sources reconstructed by sLORETA, and Fig. 5(c) shows the image reconstructed by SSLOFO. The primary activated areas are more accurately represented by SSLOFO.

Localization accuracy is a primary concern in many applications of inverse problems. One way to demonstrate localization accuracy is to test the localization error and energy error for a point source at each node in the model. A small energy error combined with a small localization error indicates a faithful reproduction of a point source. A small localization error combined with a large energy error (approaching unity) indicates that the peak of the inverse is located near the point source, but energy has spread to other locations. Our definitions of localization error and energy error can be found in [19].

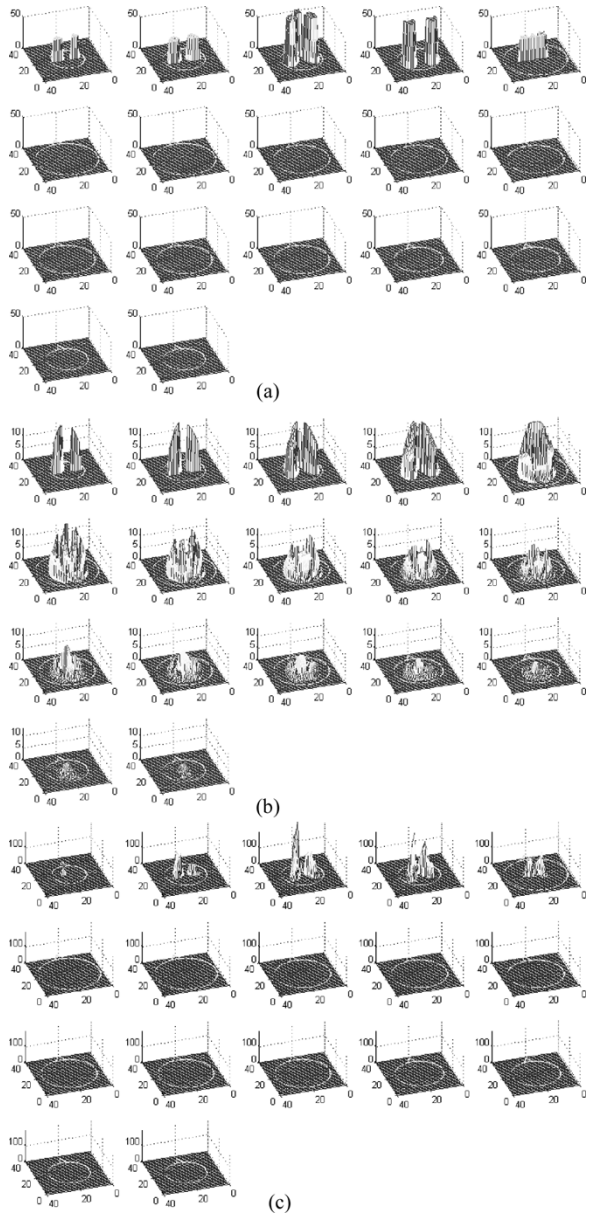

Fig. 5. Reconstruction of extended source distribution by low-resolution method and high-resolution method. (a) The simulated source configuration; (b) solution of sLORETA; (c) solution of SSLOFO.

The results of localization and energy error are listed in Table I. $\bar{E}_{\mathrm{loc}}$ denotes the mean localization error over all nodes and $E_{\max\_\mathrm{loc}}$ denotes the maximum localization error among all nodes. The third row lists the standard deviation (STD) of localization errors. $\bar{E}_{\mathrm{enrg}}$ denotes the mean energy error over all nodes and $E_{\max\_\mathrm{enrg}}$ denotes the maximum energy error among all nodes. The standard deviation of energy errors are shown in the last row. This table shows that the mean localization error of the SSLOFO algorithm is zero with a mean energy error of only 2.99%. For single source, the mean localization error of sLORETA is also zero but the mean energy error is 99.55%. This is because the image reconstructed by sLORETA

TABLE I
COMPARISON OF LOCALIZATION ABILITY OF FOUR INVERSE ALGORITHMS

	WMN	sLORETA	FOCUSS	SSLOFO
$\overline{E}_{loc}$ (*mm*)	20.05	0	2.33	0
$E_{\max\_loc}$ (*mm*)	81.03	0	38.34	0
STD of localization errors (*mm*)	12.57	0	4.50	0
$\overline{E}_{enrg}$ (%)	96.16	99.55	8.44	2.99
$E_{\max\_enrg}$ (%)	99.78	99.85	76.54	40.78
STD of energy errors (%)	3.37	0.21	20.62	5.36

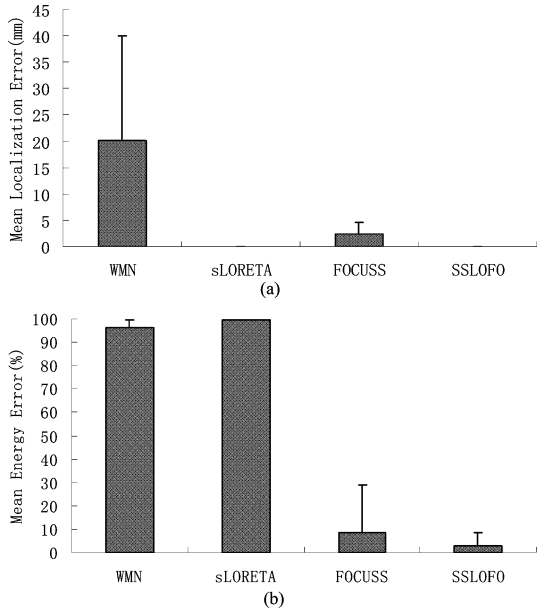

Fig. 6. (a) Mean value and standard deviation of localization error of four algorithms (b) Mean value and standard deviation of energy error of four algorithms.

has low resolution, with a large point spread function. The mean energy error of FOCUSS is 8.44% while the mean localization error is 2.33 mm. It can be inferred that FOCUSS also has good performance in recovering single sources, but our earlier results show that SSLOFO has advantages with multiple regions of localized sources. WMN has much larger localization and energy errors. The mean and standard deviation of these errors are plotted in Fig. 6, showing that SSLOFO demonstrates superior performance in both categories even for single sources. This indicates that it can reconstruct the sources correctly and robustly.

C. Simulation With Noisy Data

All of the preceding studies were performed in the absence of measurement noise. Experimental data will inevitably be contaminated by "noise" from various sources, including measurement noise and background brain activity. Because the

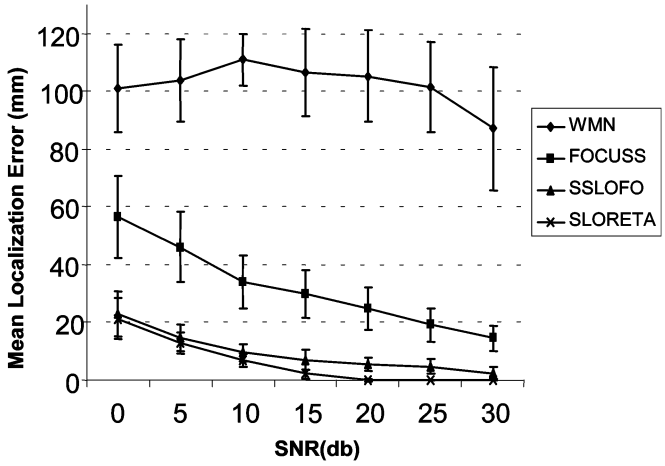

Fig. 7. Localization error of four inverse algorithms in the spherical head model with different noise levels.

EEG inverse problem is underdetermined and ill-posed, a small perturbation in the measurement can cause large changes in the solution. The technique of regularization can be used to prevent the large number of degrees of freedom in the source space from being used to over-fit to added noise. Tikhonov-Phillips regularization and truncated singular value decomposition (TSVD) are two approaches that may be used [29]–[31]. We used Tikhonov-Philips regularization in the sLORETA stage of SSLOFO. TSVD was then employed at each iteration of standardized FOCUSS to exclude the smallest singular values, with the cutoff point determined using the L-curve method [31].

In order to compare the localization ability of WMN, sLORETA, FOCUSS, and SSLOFO at different noise levels, a single point source with random orientation was placed at each of the 2394 nodes of the spherical head model and the EEG measurements were simulated. Gaussian white noise was added to the simulated measurements and the inverse solutions were computed using the above four algorithms. In this study, we increase the SNR from 0 dB to 30 dB in 5-dB increments. The SNR was defined as

$$10\log\left(\frac{\mathrm{var}(\mathbf{\Phi}_{\mathrm{exact}})}{\sigma^2}\right) \tag{19}$$

where $\mathrm{var}(\mathbf{\Phi}_{\mathrm{exact}})$ is the variance of the simulated noise-free measurements, and σ^2 is the variance of the added noise, $\mathbf{e}$, which was independent and identically distributed (IID) on each channel. The mean and standard deviation of the localization errors were computed over these 2394 simulations and are plotted versus SNR in Fig. 7. It can be seen WMN and FOCUSS have large localization errors. For single source localization, sLORETA has smaller localization error compared to SSLOFO, especially when the SNR is high. This result reflects that SSLOFO seeks a tradeoff between the spatial resolution and the precision of localization. Nevertheless, SSLOFO only produced a localization error of 7 mm at a SNR of 15 db, which is just one inter-grid distance in the cortical samples.

To evaluate the potential of our algorithm in experimental human research, a realistic head model is used in the following studies. Fig. 8(a) illustrates two groups of sources simulated in the realistic head model. Six sources were placed in the frontal

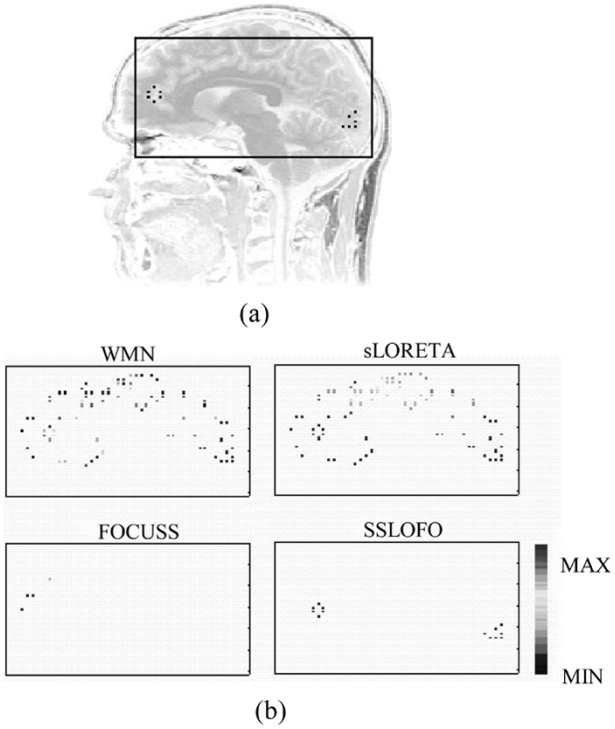

Fig. 8. Reconstruction of shaped source distribution in the realistic head model (a) the simulated source configuration; (b) solutions of four inverse algorithms.

lobe and formed a circular shape and another six sources were placed in the occipital area in the shape of a triangle. Noise was then added to simulated measurements with a SNR of 10 dB. Fig. 8(b) displays the sources estimated by WMN, sLORETA, FOCUSS, and SSLOFO. Only the plane of the sources is shown here. It can be seen that WMN and sLORETA both produced very blurred images while FOCUSS produced an over-focal image. Only SSLOFO correctly recovered the complex source distribution.

Spatio-temporal analysis of EEG is the trend in brain function research. In the following study, we compare the performance of four inverse algorithms in revealing the source waveforms. Two segments of intracranial EEG recorded from the cortex of an epileptic patient are used as the temporal waves for three simulated sources in the realistic head model. Source1 and Source2 are close to each other; the distance between them is 21 mm. Source3 is located far from Source1 and Source2, at a distance of 42 and 34 mm, respectively. In this simulation, Source2 and Source3 are synchronous sources that have identical waveforms. The EEG segments are 500 ms in length with a sample rate of 100 Hz. Noise was added to the scalp measurements with a SNR of 20 dB. Fig. 9 illustrates the original source waves and the waves revealed by WMN, sLORETA, FOCUSS, and spatio-temporal SSLOFO, respectively. The correlation coefficients between the original waveforms and the reconstructed waveforms were calculated and are listed in Table II. Spatio-temporal SSLOFO produced three waves very similar to the original source waveforms, with correlation coefficients of 0.79, 0.97, and 0.96, respectively. WMN produced three waves with correlation coefficients of 0.18, 0.95, and 0.99. However, the temporal reconstructions at

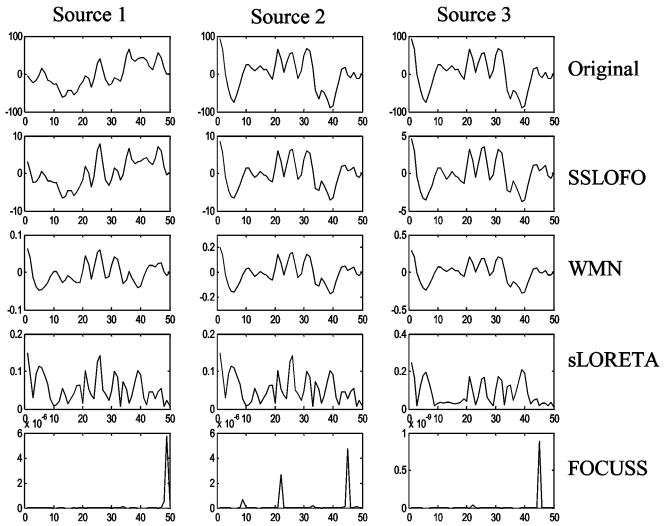

Fig. 9. Reconstruction of source waveforms. Three columns represent waves on three source locations. The first row represents the original waveforms simulated on the sources. Source2 and Source3 are 100% correlated. The following four rows represent waveforms reconstructed by different inverse algorithms.

TABLE II
CORRELATION COEFFICIENTS BETWEEN THE SIMULATED SOURCE WAVES AND RECONSTRUCTED WAVES BY FOUR INVERSE ALGORITHMS

	Source wave 1	Source wave 2	Source wave 3
SSLOFO	0.79	0.97	0.96
WMN	0.18	0.95	0.99
sLORETA	-0.02	0. 06	-0.06
FOCUSS	-0.05	0.24	0.11

the two close locations (Source1 and Source2) are almost the same; this indicates the temporal activities of these two sources have been mixed. Though sLORETA is a nonlinear method, it has very wide point-spread function so it can recover the temporal waveforms to some extent. Because of standardization, sLORETA provides the power of the current sources rather than current density. So the waves produced by sLORETA are quite different from the originals. However, for a fair comparison, we calculated the correlation coefficients between the power of originals and the waves given by sLORETA. Similar to WMN, the reconstructions for source 1 and 2 resemble one other. This is understandable because low spatial resolution methods such as sLORETA and WMN are not able to separate two close sources with different activities. As we have discussed above, FOCUSS usually cannot produce a continuous wave, as illustrated in Fig. 9.

IV. DISCUSSION

When implementing SSLOFO, some parameters should be selected according to specific requirements. In this recursive process, we define a neighboring region around each prominent node and carry out a smoothing operation within this region

[19]. This region should not be too large, because a large neighborhood may cause the solution of each step being overly smoothed, resulting in an early exit because of region growth. In our simulations, the region was set to be a sphere with a radius of two grid units in the model space. This neighboring region can have other shapes, e.g., an ellipsoid as employed by shrinking ellipsoid algorithm [32]. It might also be feasible to set the size dynamically, according to the source magnitudes in the current inverse, but we have not investigated that possibility. Another parameter is the threshold for excluding weak source nodes at each step. A high threshold can speed up the algorithm but may cause the loss of meaningful nodes. In our studies, we excluded those sources with amplitude less than 1% of the maxima in the image. If the sources are few and focal, the threshold can be raised to speed up convergence, but, based on our experience, we would not suggest that a threshold higher than 5% when there is no prior knowledge of the underlying sources. Another important problem in the application of this algorithm to human research is defining the stopping criterion according to specific needs. We can cease the iterations when the maximum current density of the solution exceeded a threshold. The maximum allowable cortical current density could be estimated from published experimental studies [32]–[34]. The threshold can also depend on specific objectives of the work, e.g., if the data to be processed are evoked potentials extracted from the EEG, or spontaneous EEG collected during epileptic seizures. Stopping the process earlier will generally produce an image reflecting the general areas of activity, while a more fully iterated process will produce a more focal solution. Regularization is another issue that deserves further consideration. SSLOFO employs Tikhonov regularization in the sLORETA computations and TSVD in the FOCUSS computations. Tikhonov regularization demands less computation effort and works well in sLORETA, but is not as effective as TSVD in FOCUSS [16]. The TSVD regularization parameter is usually determined by the L-curve method. However, it should be noted that L-curve does not always find the optimal parameter. A method that can robustly estimate the noise level of the real data will greatly help in finding the best regularization parameter. As such a method remains an open topic in research, preprocessing of the EEG data before the inverse calculation is highly preferred.

The inverse problem has no unique solution and various constraints can be used to produce a physiologically meaningful source image. Low-resolution methods such as LORETA, sLORETA, and WMN can estimate the area of primary activity but suffer from the poor spatial resolution. These inverse methods are useful in reconstructing some simple source configurations but become inefficient for large numbers of sources that are not restricted to a given area. The large point spread functions of these techniques can make it difficult to discern multiple active regions. High-resolution methods such as FOCUSS are able to localize focal sources which relate to some specific diseases or functions of the brain, but these methods are not generally robust to distributed activity and may generate "over-focal" results. It should also be emphasized that "high resolution" is not necessarily better than "low resolution." Since the extent of the brain sources may vary in different experiments, both low-resolution methods and high-resolution methods have their own appropriate applications.

So far most inverse methods favor one of these two extremes: either a few clustered sources or a low-resolution rendering of primary regions of activity. In this context, we would like to cite a paragraph from [16]. "Although neuromagnetic activity is believed to be often localized, distributed patterns of activity are also known to exist, for example in epileptic seizures. Given the severely underdetermined nature of the neuromagnetic imaging problem, an inverse method can only provide solutions that fit its specific objectives, e.g., reconstructing localized versus extended sources… Although a trade off between methods with different model objectives for different extents of the source activity can be attempted, we expect that in the future, successful methods in magnetoencepalography will rely on combining a number of algorithms in a single procedure." Recent development in brain mapping techniques has proven the efficiency of the combining strategy [11], [15]. By taking fMR images as the *a priori* constraint of the EEG/MEG inverse problem [11], or by combining L1-norm with L2-norm methods [15], compromise between focal sources and smooth distribution has been achieved.

It is, of course, possible for an investigator to manually try several approaches and interpret the results accordingly. SSLOFO is a modest attempt to combine the advantages of both low- and high-resolution methods in an automated fashion, although some limited knowledge of the situation goes into determination of a couple parameters, and more study on the effect of those is certainly warranted. Starting from a very smooth estimate, SSLOFO improves the spatial resolution using the recursive strategy of FOCUSS. A very important process termed standardization is applied in order to keep the estimate localized on regions with significant activity, although multiple regions may emerge. The algorithm is further improved by automatically adjusting the source space. Our simulations show that SSLOFO combines the features of high and low resolutions methods. It can extract regions of dominant activity while simultaneously localizing multiple sources within those regions. The algorithm successfully reconstructed source configurations with different shapes, and outperformed the low-resolution methods in reconstructing some distributed sources. More importantly, the adaptive definition of the solution space in SSLOFO enables a convenient way to integrate temporal information. Through a simple re-weighting strategy, the source information derived from the nonlinear algorithm at each time sample is incorporated into a linear process. This spatio-temporal version of SSLOFO is able to reveal different waveforms at close locations. This feature is especially useful when temporal information studies such as phase synchrony, nonlinear dynamics or spectrum analysis are performed on the sources.

ACKNOWLEDGMENT

The authors would like to thank R. D. Pascual-Marqui and J. Haueisen for providing the data of the head models.

REFERENCES

[1] M. Scherg and D. von cramon, "Two bilateral sources of the late AEP as identified by a spatio-temporal dipole model," *Electroenceph.Clin. Neurophysiol*, vol. 62, pp. 290–299, 1985.

[2] R. M. Leahy *et al.*, "A study of dipole localization accuracy for MEG and EEG using a human skull phantom," *Electroenceph.Clin. Neurophysiol.*, vol. 107, no. 2, pp. 159–73, 1998.

[3] B. N. Cuffin, "EEG dipole source localization," *IEEE Eng. Med. Biol. Mag.*, vol. 17, no. 5, pp. 118–122, Sep.-Oct. 1998.

[4] J. C. Mosher, P. S. Lewis, and R. M. Leahy, "Multiple dipole modeling and localization from spatio-temporal MEG data," *IEEE Trans. Biomed. Eng.*, vol. 39, no. 6, pp. 541–557, Jun. 1992.

[5] J. C. Mosher and R. M. Leahy, "Recursive MUSIC: A framework for EEG and MEG source localization," *IEEE Trans. Biomed. Eng.*, vol. 45, no. 11, pp. 1342–1354, Nov. 1998.

[6] T. R. Knosche, E. M. Berends, H. R. Jagers, and M. J. Peters, "Determining the number of independent sources of the EEG," *Sim. Study Inf. Criteria: Brain Topogr.*, vol. 11, no. 2, pp. 111–124, 1998.

[7] C. H. Wolters, R. F. Beckmann, A. Rienacker, and H. Buchner, "Comparing regularized and nonregularized nonlinear dipole fit methods: A study in a simulated sulcus structure," *Brain Topogr.*, vol. 12, no. 1, pp. 3–18, 1999.

[8] R. D. Pascual-Marqui, C. M. Michel, and D. Lehmann, "Low resolution electromagnetic tomography: A new method for localizing electrical activity in the brain," *Int. J. Psychophysiol.*, vol. 18, pp. 49–65, 1994.

[9] R. D. Pascual-Marqui, "Review of methods for solving the EEG inverse problem," *Int. J. Bioelectromagn.*, vol. 1, pp. 75–86, 1999.

[10] M. Fuchs, M. Wagner, T. Kohler, and H. Wischmann, "Linear and nonlinear current density reconstructions," *J. Clin. Neurophysiol.*, vol. 16, no. 3, pp. 267–295, 1999.

[11] A. M. Dale, A. K. Liu, B. R. Fischl, R. L. Buckner, J. W. Belliveau, J. D. Lewine, and E. Halgren, "Dynamic statistical parametric neurotechnique mapping: Combining fMRI and MEG for high-resolution image of cortical activity," *Neuron*, vol. 26, pp. 55–67, 2000.

[12] J. Mosher, S. Baillet, and R. Leahy, "Equivalence of linear approaches in bioelectromagnetic inverse solutions," in *Proc. IEEE Workshop on Statistical Signal Processing*, Sep.-Oct. 2003, pp. 294–297.

[13] M. S. Hämäläinen, "Magnetoencephalography—Theory, instrumentation, and applications to noninvasive studies of the working human brain," *Rev. Mod. Phys.*, vol. 65, no. 2, pp. 413–497, 1993.

[14] R. D. Pascual-Marqui, "Standardized low resolution brain electromagnetic tomography(sLORETA): Technical details," *Meth. Findings Exp. Clin. Pharmacol.*, vol. 24D, pp. 5–12, 2002.

[15] K. Uutela, M. Hämäläinen, and E. Somersalo, "Visualization of magnetoencephalographic data using minimum current estimates," *NeuroImage*, vol. 10, pp. 173–80, 1999.

[16] I. F. Gorodnitsky, J. S. George, and B. D. Rao, "Neuromagnetic source imaging with FOCUSS: A recursive weighted minimum norm algorithm," *Electroenceph. Clin. Neurophysiol.*, vol. 95, pp. 231–251, 1995.

[17] I. F. Gorodnitsky and B. D. Rao, "Sparse signal reconstruction from limited data using FOCUSS: a re-weighted minimum norm algorithm," *IEEE Trans. Signal Process.*, vol. 45, no. 3, pp. 600–616, Mar. 1997.

[18] H. Liu and F. Yang, "An approach to achieve concentrated 3-D spatio-temporal EEG pattern inside brain," presented at the Annu. Conf. Biomedical Electronics, Wuhan, China, 2001.

[19] H. Liu, X. Gao, P. Schimpf, F. Yang, and S. Gao, "A recursive algorithm for the three-dimensional imaging of brain electric activity: shrinking LORETA-FOCUSS," *IEEE Trans. Biomed. Eng.*, vol. 51, no. 10, pp. 1794–1802, Oct. 2004.

[20] B. D. Van Veen, W. van Drongelen, M. Yuchtman, and A. Suzuki, "Localization of brain electrical activity via linearly constrained minimum variance spatial filtering," *IEEE Trans. Biomed. Eng.*, vol. 44, no. 9, pp. 867–880, Sep. 1997.

[21] U. Schmitt, A. K. Louis, C. H. Wolters, and M. Vauhkonen, "Efficient algorithms for the regularization of dynamic inverse problems: II. Applications," *Inverse Prob.*, vol. 18, no. 3, pp. 659–676, 2002.

[22] P. C. Hansen, *Rank-Deficient and Discrete Ill-Posed Problems*. Philadelphia, PA: SIAM, 1998.

[23] J. Talairach and P. Tournoux, *Co-Planar Stereotaxic Atlas of the Human Brain*. Stuttgart, Germany: Thieme, 1988.

[24] N. Shrinidhi, D. R. Haynor, Y. Wang, D. B. Joregenson, G. H. Bardy, and Y. Kim, "An efficient tissue classifier for building patient-specific finite element models from X-ray CT images," *IEEE Trans. Biomed. Eng.*, vol. 43, no. 3, pp. 333–337, Mar. 1996.

[25] A. Geddes and L. E. Baker, "The specific resistance of biological material—A compendium of data for the biomedical engineer and physiologist ," *Med. Biol. Eng.*, vol. 5, pp. 271–293, 1967.

[26] P. Schimpf, J. Haueisen, C. Ramon, and H. Nowak, "Realistic computer modeling of electric and magnetic fields of human head and torso," *Parallel Comput.*, vol. 24, pp. 1433–1460, 1998.

[27] D. Weinstein, L. Zhukov, and C. Johnson, "Lead-field bases for electroencephalography source imaging," *Ann. Biomed. Eng.*, vol. 28, no. 9, pp. 1059–1066, 2000.

[28] C. H. Wolters, L. Grasedyck, and W. Hackbusch, "Efficient computation of lead field bases and influence matrix for the FEM-based EEG and MEG inverse problem," *Inverse Prob.*, vol. 20, no. 4, pp. 1116–1099, 2004.

[29] A. N. Tikhonov and V. Y. Arsenin, *Solution of Ill-Posed Problems*. New York: Wiley, 1977.

[30] I. Iakovidis and R. M. Gulrajani, "Improving tikhonov regularization with linearly constrained optimization: Application to the inverse epicardial potential solution," *Math. Biosci.*, vol. 112, pp. 55–80, 1992.

[31] P. C. Hansen and D. P. O'Leary, "The use of the L-curve in the regularization of discrete ill-posed problems," *SIAM J. Scientific Comput.*, vol. 14, pp. 1487–1503, 1993.

[32] R. Srebro, "Iterative refinement of the minimum norm solution of the bioelectric inverse problem," *IEEE Trans. Biomed. Eng.*, vol. 43, no. 5, pp. 547–552, May 1996.

[33] A. T. Kulics and L. J. Cauller, "Cerebral cortical somatosensory evoked responses, multiple unit activity and current-source densities," *Exp. Brain Res.*, vol. 62, pp. 46–60, 1986.

[34] L. J. Cauller and D. T. Kulics, "The neural basis of the behaviorally relevant N1 component of the somatosensory-evoked potential in S1 cortex of awake monkeys," *Exp. Brain Res.*, vol. 84, pp. 607–619, 1991.

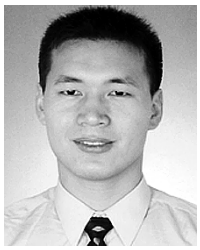

Hesheng Liu (M'04) was born in Fukien, China, in 1975. He received the B.S. degree and Ph.D. degree in biomedical engineering from Tsinghua University, Beijing, China, in 1997 and 2003, respectively.

His research interests include EEG/MEG inverse problem, brain-computer interface, epileptic seizure detection and prediction, electrical impedance tomography, and pattern recognition.

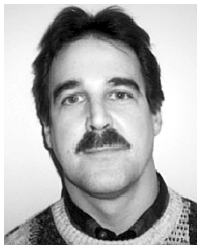

Paul H. Schimpf (S'94–M'95) received the B.S.E.E. (summa cum laude), M.S.E.E., and Ph.D. degrees from the University of Washington, Seattle, in 1982, 1987, and 1995.

He is currently an Associate Professor in the School of Electrical Engineering and Computer Science at Washington State University, Spokane, and coordinates the Computer Engineering Program. He teaches upper division and graduate courses in digital systems design, computer architecture, computer programming, and computational electromagnetics. His research interests include numerical methods for forward and inverse solutions to partial differential equations over complex heterogeneous domains.

Guoya Dong received the Ph.D. in biomedical engineering from Tsinghua University, Beijing, China, in 2003. She is currently doing post-doctoral research work in Province-ministry Joint Key Laboratory of Electromagnetic Field and Electrical Apparatus Reliability, Department of Electrical Engineering, Hebei University of Technology, Tianjin, China.

Her basic research interests are electrical impedance tomography, inverse problem, numerical methods for forward problem including finite volume method, finite element method and boundary element method.

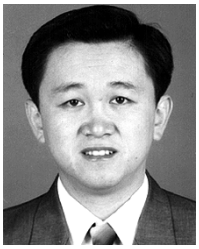

Xiaorong Gao was born in Beijing, China, in 1963. He received the B.S. degree in biomedical engineering from Zhejiang University, Hangzhou, China, in 1986, the M.S. degree in biomedical engineering from Peking Union Medical College, Peking, China, in 1989, and the Ph.D. degree in biomedical engineering from Tsinghua University, Beijing, China, in 1992.

He has been working in Tsinghua University since 1992 at the Department of Electrical Engineering and Department of Biomedical Engineering. His current research interests are biomedical signal processing and medical instrumentation.

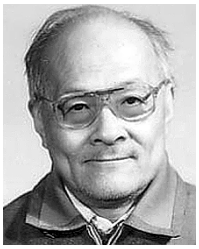

Fusheng Yang received the B.Sc. degree in electrical engineering from Amoy University, Fukien, China, in 1949.

Since 1951, he has been a Faculty Member of the Department of Electrical Engineering of Tsinghua University, Beijing, China, where he has held the rank of Professor since 1980. He is the author of *Biomedical Signal Processing* (China: Higher Education Press, 1989) and *Engineering Analysis of Wavelet Transform and Its Application* (China: Science Press, 1998). His current research interest lies mainly in the application of spatial analysis, time-frequency, time-scale analysis, and nonlinear dynamics analysis to biomedical signals.

Shangkai Gao (SM'93) graduated in electrical engineering and received the M.E. degree of biomedical engineering in Tsinghua University, Beijing, China, in 1970 and 1982, respectively.

From 1984 to 1985 she worked in the Department of Electrical Engineering and Computer Science at the George Washington University, Washington, DC, as a Visiting Scholar. She is currently a Professor with the Department of Biomedical Engineering, Tsinghua University. Her research interests include biomedical signal processing and medical ultrasound.

Prof. Gao in an Associate Editor of IEEE TRANSACTION ON BIOMEDICAL ENGINEERING.